



Lewis Research Center
IN-32-12
169399
438

Material Parameter Determination from Scattering Measurements

by

A. Dominek, A. Park and L. Peters, Jr.

The Ohio State University
ElectroScience Laboratory

Department of Electrical Engineering
Columbus, Ohio 43212

Technical Report No. 719300-3
Grant No. NAG3-784
September 1988

National Aeronautics and Space Administration
Lewis Research Center
21000 Brookpark Rd.
Cleveland, OH 44135

(NASA-CR-183312) MATERIAL PARAMETER
DETERMINATION FROM SCATTERING MEASUREMENTS
(Ohio State Univ.) 43 P CSCI 20N

N89-10225

Unclas
G3/32 0169399

NOTICES

When Government drawings, specifications, or other data are used for any purpose other than in connection with a definitely related Government procurement operation, the United States Government thereby incurs no responsibility nor any obligation whatsoever, and the fact that the Government may have formulated, furnished, or in any way supplied the said drawings, specifications, or other data, is not to be regarded by implication or otherwise as in any manner licensing the holder or any other person or corporation, or conveying any rights or permission to manufacture, use, or sell any patented invention that may in any way be related thereto.

Material Parameter Determination from Scattering Measurements

by

A. Dominek, A. Park and L. Peters, Jr.

Technical Report No. 719300-3

Grant No. NAG3-784

September 1988

National Aeronautics and Space Administration
Lewis Research Center
21000 Brookpark Rd.
Cleveland, OH 44135

Contents

List of Figures	iv
1 Introduction	1
2 Scattering Measurement Parameter Extraction	4
3 Measurement Fixtures	7
I Parallel Plate Fixture	7
II Ground Plane Fixture	10
III Sample Heating	16
4 Example Measurements and Parameter Extraction	19
5 Extraction Technique Sensitivity	29
6 An Alternate Fixture	33
7 Conclusions	36

PRECEDING PAGE BLANK NOT FILMED

List of Figures

3.1	Parallel plate test fixture.	8
3.2	Geometry for a coated cylinder.	10
3.3	Swept frequency response for a 2" diameter perfectly conducting circular cylinder. Solid line - backscatter, dashed line - 90° bistatic.	11
3.4	Swept frequency backscatter response for circular cylinders with $\epsilon_r = 24 - j2$ and $\mu_r = 2 - j.2$. Solid line - 2" diameter homogeneous cylinder, dashed line - 2" diameter perfectly conducting cylinder with .07" thick dielectric coating.	12
3.5	Ogival shaped ground plane fixture.	13
3.6	Geometry for a coated hemisphere.	16
3.7	Swept frequency response for a 2" diameter perfectly conducting hemisphere with the incident field 30° from grazing incidence. Solid line - theta polarizaton, dashed line - phi polarization.	17
3.8	Swept frequency, theta polarized backscatter response for hemispheres with $\epsilon_r = 24 - j2$ and $\mu_r = 2 - j.2$. Solid line - 2" diameter homogeneous hemisphere, dashed line - 2" diameter perfectly conducting hemisphere with .07" thick dielectric coating.	18
4.1	Scattering time signature of parallel plate fixture illustrating the scattering terms present for a reflection measurement.	20
4.2	Scattering time signature of parallel plate fixture illustrating the scattering terms present for a reflection measurement after background subtraction.	21

4.3	Parallel plate swept frequency results for a 3" diameter perfectly conducting disk: Solid - measured, dashed - calculated. a) Backscatter. b) bistatic, angle of 110°.	23
4.4	Measured parallel plate swept frequency results for a 2" diameter Teflon disk. Solid - backscatter, dashed - bistatic, angle of 110°.	24
4.5	Extracted constitutive parameters for a 2" diameter Teflon disk.	25
4.6	Ground plane swept frequency results for a 2" diameter perfectly conducting hemisphere, 30° from grazing: Solid - measured, dashed - calculated. a) Theta polarization. b) Phi polarization.	26
4.7	Measured ground plane swept frequency results for a 2" diameter Plexiglas hemisphere, 30° from grazing. Solid -theta polarization, dashed - phi polarization.	27
4.8	Extracted constitutive parameters for a 2" diameter Plexiglas hemisphere.	28
5.1	Normalized extracted constitutive parameters from calculated scattered field values. Assumed diameter for the perfectly conducting hemisphere: Solid line - 2 % smaller, dashed line - 2 % larger.	31
5.2	Backscattered results for a 2" diameter Teflon disk in the parallel plate fixture. Normalized extracted permittivity: Solid line - 31 points, dashed line - 71 points.	32
6.1	An alternate fixture using a rectangular waveguide fixture and a planar fixture sample.	35

Chapter 1

Introduction

The electrical, macroscopic performance of isotropic material can generally be described through their constitutive scalar parameters, permittivity and permeability which are symbolically represented by ϵ and μ , respectively. These parameters relate the electric and magnetic flux densities to the electric and magnetic fields through the following relationships:

$$\mathbf{D} = \epsilon \mathbf{E} \tag{1.1}$$

and

$$\mathbf{B} = \mu \mathbf{H}. \tag{1.2}$$

It is through these parameters that the interaction of electromagnetic waves with material can be quantized in terms of reflection and transmission coefficients, and propagation and attenuation factors.

These parameters can be complex which indicates the loss component of the material. The loss is represented in the imaginary part of the parameters as $\epsilon = \epsilon' - j\epsilon'' = \epsilon_0 \epsilon_r$ and $\mu = \mu' - j\mu'' = \mu_0 \mu_r$ where the subscripts o and r refer to the free space and relative values. When the loss mechanism is conductive in nature, ϵ'' is replaced with σ/ω where σ is the conductivity

of the material and ω is the radian frequency. Often, the loss is stated as loss tangents being $\tan \delta_e = \epsilon''/\epsilon'$ and $\tan \delta_m = \mu''/\mu'$.

The acquisition of constitutive material parameters are often obtained from reflection and transmission measurements using a coaxial or waveguide fixture with an internal material sample. The parameters are then recovered from exact expressions relating the measured quantities to the parameters. Obviously, the number of unknowns determine the number of independent measurements required. The most convenient measurements are reflection and transmission for such closed (nonradiating) fixtures. Accurate parameters are difficult to obtain when the material can not be shaped into the desired shapes resulting in undesirable air gaps between the sample and fixture.

Alternate techniques have been examined to acquire the necessary number of independent measurements. The goal has been to develop a technique to conveniently measure material samples at high temperatures (greater than 800° F) over a broadband of frequencies (2-18 GHz) to determine the constitutive material parameters. The simplest approach examined was to measure the reflected field as a function of frequency from a waveguide aperture terminated with a material coated planar conductor. This approach would be very desirable since planar material samples can readily be fabricated. Although the measured reflected field varied between samples and sample temperature, there were deficiencies. Since only one measurement was possible (reflection), another independent quantity had to be generated. One approach was to differentiate or integrate around the desired frequency of interest to form another entity. This approach had reasonable success [1] where the measurement entailed a free space quantity and a good analytical representation of the scattered fields was known. This approach was not successful in this case primarily because a sufficient model of the reflected field was not readily available. Another potential limitation for

this approach is that the second entity may be too similar to the measured quantity to form a second independent entity.

Other alternate techniques entailed the swept frequency measurement of scattered fields in a parallel plate or ground plane fixture as described in [2]. Comparable scattering measurements for small dielectric spheres in free space to obtain the constitutive parameters have had good success [3,4]. The parallel plate or ground plane fixture offers a means to heat a sample to the desired temperature and perform broadband measurements simultaneously. A major drawback to either of these two techniques would be the fabrication of cylindrical or hemispherical material samples. In this report, parameter determination using the parallel plate and ground plane fixtures are discussed with results presented.

Chapter 2

Scattering Measurement Parameter Extraction

The method of parameter extraction from measurements is dependent upon the fixture used. Conventional coaxial and rectangular waveguide fixture uses reflection and transmission measurements in deterministic expressions to arrive at the desired parameters [5]. These expressions are available since the field behavior can be described with one mode. Performing broadband measurements involves many modes in general and a more complex procedure to extract the desired parameters. One approach involved the free space measurement of a dielectric sphere [4]. For electrically small spheres ($a \leq .2\lambda$) only two modes (dipole moments) are required to adequately describe the scattered field. As the sphere becomes electrically larger, more modes are required and accordingly more independent measurements (one measurement for each mode).

An alternate approach was taken to require only two independent measurements to arrive at the desired parameters. A search algorithm was employed to search for the unknown constitutive parameters using the measured data and analytical representation. The search algorithm adapted here was the Newton-Raphson technique. The major disadvantage for this approach is the sensitivity of the algorithm to converge due to noise in the data.

The Newton-Raphson technique iteratively solves for the unknown parameters by forcing two convenient functionals to zero. The functionals, $F_{0,1}$, for each frequency are defined to be

$$F_0 = M_0 - C_0 = 0 \quad (2.1)$$

and

$$F_1 = M_1 - C_1 = 0 \quad (2.2)$$

where the $M_{0,1}$ and $C_{0,1}$ are the independent measured and calculated responses for the sample geometry. The calculated responses are dependent upon the parameters ϵ and μ which are iteratively varied until some minimum error criterion has been achieved. The unknown parameters are iterated with the following process from some initial guess

$$\epsilon_{i+1} = \epsilon_i + \Delta\epsilon_i \quad (2.3)$$

and

$$\mu_{i+1} = \mu_i + \Delta\mu_i \quad (2.4)$$

where

$$\Delta\epsilon = \frac{F_1 \frac{\partial F_0}{\partial \epsilon} - F_0 \frac{\partial F_1}{\partial \epsilon}}{J} \quad (2.5)$$

and

$$\Delta\mu = \frac{F_0 \frac{\partial F_1}{\partial \mu} - F_1 \frac{\partial F_0}{\partial \mu}}{J} \quad (2.6)$$

and

$$J = \begin{vmatrix} \frac{\partial F_0}{\partial \epsilon} & \frac{\partial F_0}{\partial \mu} \\ \frac{\partial F_1}{\partial \epsilon} & \frac{\partial F_1}{\partial \mu} \end{vmatrix}. \quad (2.7)$$

Reliable results can be obtained if accurate measurements are made. The collection of these measurements are facilitated with the HP-8510B Network Analyzer. This computer controlled device can readily perform reflection and transmission measurements between 2 and 18 GHz. A very desirable feature of swept frequency measurements, which the HP-8510B incorporates through software, is the time gating of undesired signals from a desired signal. This time gating eliminates error terms that originate from other scattering centers located away from the desired scattering center. Such potential error signals are due to scattering from fixture terminations which are not included in the analytical model.

The measurements obtained have to be calibrated before they can be used in the search algorithm. The calibration entails the minimization of scattering which is not sample dependent and the frequency correction of the system response. The measurements required are the frequency responses for when the unknown sample is in the fixture and when it is absent from the fixture along with the frequency response for a known sample (reference) which is usually a perfectly conducting sample. This measurement data is then used in the following formula to obtain calibrated data

$$\text{CSD} = \left(\frac{\text{MSD} - \text{MBD}}{\text{MRD} - \text{MBD}} \right) \text{CRD} \quad (2.8)$$

where CSD is calibrated sample data, MSD is measured sample data, MBD is measured background data, MRD measured reference data and CRD is calculated (exact) reference data. The subtraction process in the above equation minimizes the influence of other scattering centers that are not sample dependent. The system response is normalized from the measurement through the scaling of the sample response with the measured and calculated responses for the reference.

Chapter 3

Measurement Fixtures

Of the possible fixtures that would allow the samples to be heated without disturbing the measurements and having an exact analytical scattered field representation for the sample are the parallel plate waveguide and shaped ground plane fixtures. Such fixtures were fabricated based upon electromagnetic constraints given in [2] and room temperature measurements were performed to evaluate these fixtures.

The consideration of sample size for these fixtures is that the sample can be heated uniformly and the electrical thickness is sufficient to permit a significant field interaction to occur. If the sample is supported on a conductive substrate and the coating thickness is too thin, the scattered field will be influenced more by the substrate parameter (its radius) and not by the material's constitutive parameters.

I Parallel Plate Fixture

The parallel plate fixture is simply a parallel plate waveguide which will allow an electric field to propagate between the plates to illuminate a sample. Figure 3.1 illustrates the fixture which was built using a wood frame and aluminium sheeting to form the conductive sheets. The fixture has two tapered sections attached to an interior region which the sample is measured in. The tapered sections allow the electric field to be directed to

and from the interior region for monostatic and bistatic reflection measurements. The vertices of the tapered feed sections have a coaxial port which permits a connection to the HP-8510B Network Analyzer. It is extremely important to physically position the coaxial port as close to the vertex as possible to minimize an undesired reflection coming from the vertex. The spacing between the parallel plates was chosen to allow only the dominant mode to propagate in this structure between 2 and 18 GHz.

The canonical sample shape is a circular cylinder which should maintain a tight physical contact between the ends of the cylinder and the aluminium plates. Any gap between the plates and sample will result in error in the measurement. For even sample heating, the material under test could be coated onto a hollow tube with internal electric heating coils.

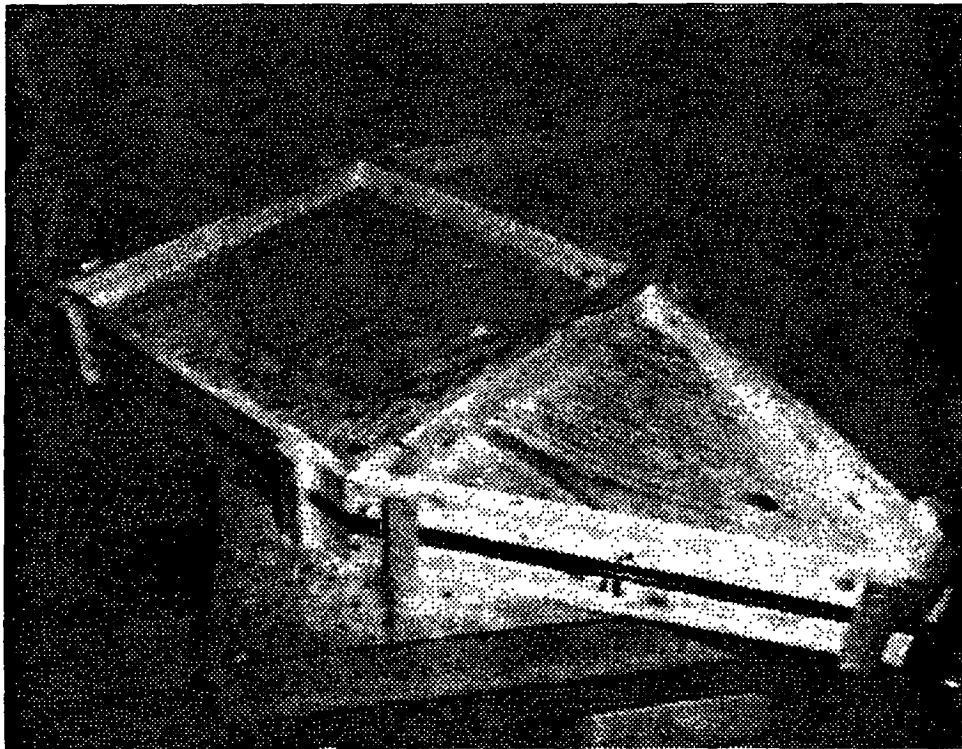


Figure 3.1: Parallel plate test fixture.

The exact scattered fields for the dielectric circular cylinder or a coated

perfectly conducting circular cylinder are readily calculated by eigenfunction expressions. The geometry for a coated perfectly conducting circular cylinder is shown in Figure 3.2. The scattered far field for plane wave illumination is given by [6]

$$E_z^s = E_z^i \sqrt{\frac{2}{\pi}} e^{j\frac{\pi}{4}} \frac{e^{-jk\rho}}{\sqrt{k\rho}} \sum_{n=0}^{\infty} a_n \cos n\left(\frac{\pi}{2} - \phi\right) \quad (3.1)$$

where a_n are ratios of cylindrical Bessel functions, J_n , N_n and $H_n^{(2)}$ and given by

$$a_n = -\epsilon_n \frac{J_n'(kb) - Z_n J_n(kb)}{H_n^{(2)'}(kb) - Z_n H_n^{(2)}(kb)} \quad (3.2)$$

and

$$Y_n = \eta_r^{-1} \frac{J_n(k_1 a) N_n'(k_1 b) - N_n(k_1 a) J_n'(k_1 b)}{J_n(k_1 a) N_n(k_1 b) - N_n(k_1 a) J_n(k_1 b)} \quad (3.3)$$

where $\eta_r = \sqrt{\frac{\mu_r}{\epsilon_r}}$ is the relative wave impedance of the material coating and $k_1 = \sqrt{\epsilon_r \mu_r} k$ and k is the free space wave number. The parameter ϵ_n is equal to unity for $n = 0$ and 2 for $n \neq 0$.

These above expressions reduce to simpler forms for special cases. The quantity Y_n is equal to

$$\eta_r^{-1} \frac{J_n'(k_1 b)}{J_n(k_1 b)}$$

for a homogeneous cylinder. Additionally, for the perfectly conducting cylinder, $Y_n = \infty$.

The 2-18 GHz swept frequency response for a 2" diameter perfectly conducting cylinder is shown in Figure 3.3 where the solid curve is the monostatic (reflection) case and the dashed is the 90° bistatic reflection case. These two cases are the nominal choices to acquire two independent

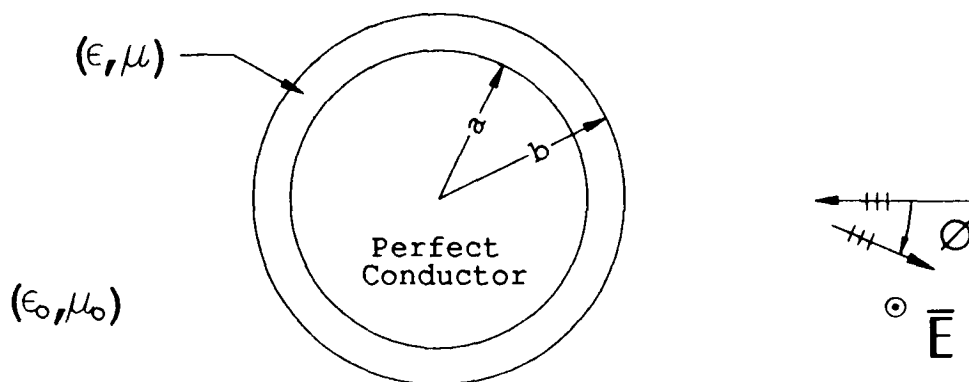


Figure 3.2: Geometry for a coated cylinder.

measurements. Note that these responses are ideal for calibration references since they are fairly constant. Figure 3.4 illustrates the backscatter frequency response for a homogeneous 2" dielectric cylinder (solid line) and a 2" diameter perfectly conducting cylinder coated with a .07" thick layer of dielectric. In both cases, the constitutive parameters are $\epsilon_r = 24 - j2$ and $\mu_r = 2 - j2$. Illustrated in this figure is the effect of loss on the scattered field for a given amount of material. For the homogeneous cylinder, the scattered field becomes solely dependent upon the reflection from the illuminated face of the cylinder as the frequency is increased. This behaviour is not the same for the hemisphere case to follow next. In this geometry, a creeping wave will exist along with the specular field.

II Ground Plane Fixture

The ground plane fixture shown in Figure 3.5 simulates an infinite conducting surface for which the scattered fields from a hemisphere can be calculated. The ogival shape controls the scattered field from the edges of the fixture. The dominant scattered fields from the fixture would be the tips which are low in value compared to those scattered from a straight edge at normal incidence. This fixture allows several different types of

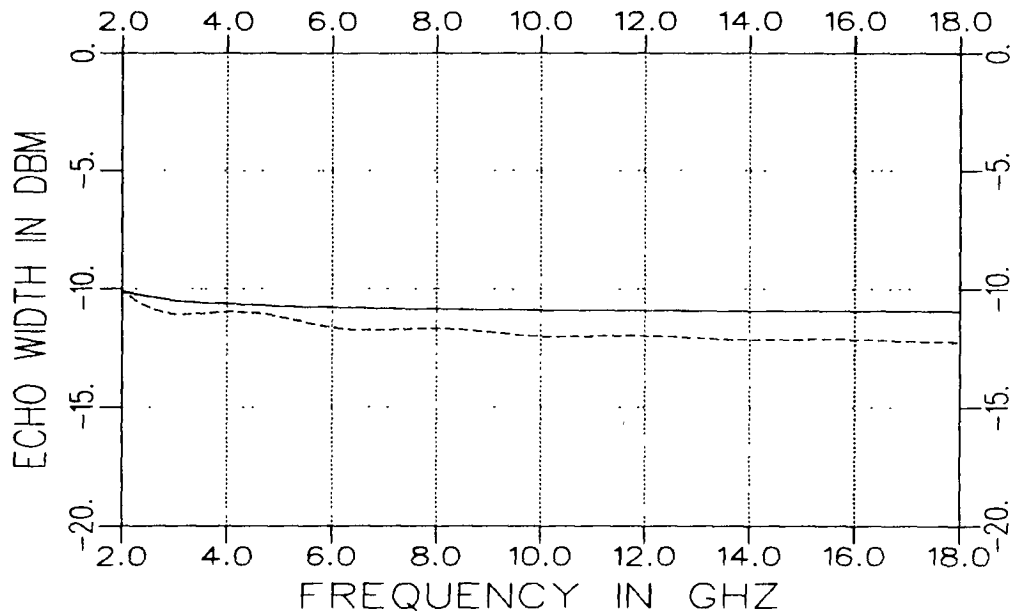


Figure 3.3: Swept frequency response for a 2" diameter perfectly conducting circular cylinder. Solid line - backscatter, dashed line - 90° bistatic.

independent measurements to be performed. The measurement depends upon the polarization of the incident field, the elevation angle of the incident field above the ground plane and the bistatic angle between the source and receiver. The most advantageous pair of measurements are when the source and receiver are located at the same point (backscatter) and both polarizations are measured for the same elevation angle. The source fields for this fixture were generated using a broadband 2-18 GHz AEL [7] horn connected to the HP-8510B Network Analyzer.

The canonical sample shape is a hemisphere which should maintain a tight physical contact to the ground plane fixture. Any gap between the ground plane and sample will result in error in the measurement. For even sample heating, the material under test could be coated onto a hollow hemisphere with internal electric heating coils or a gas burner.

The geometry of a coated dielectric hemisphere over an infinite ground

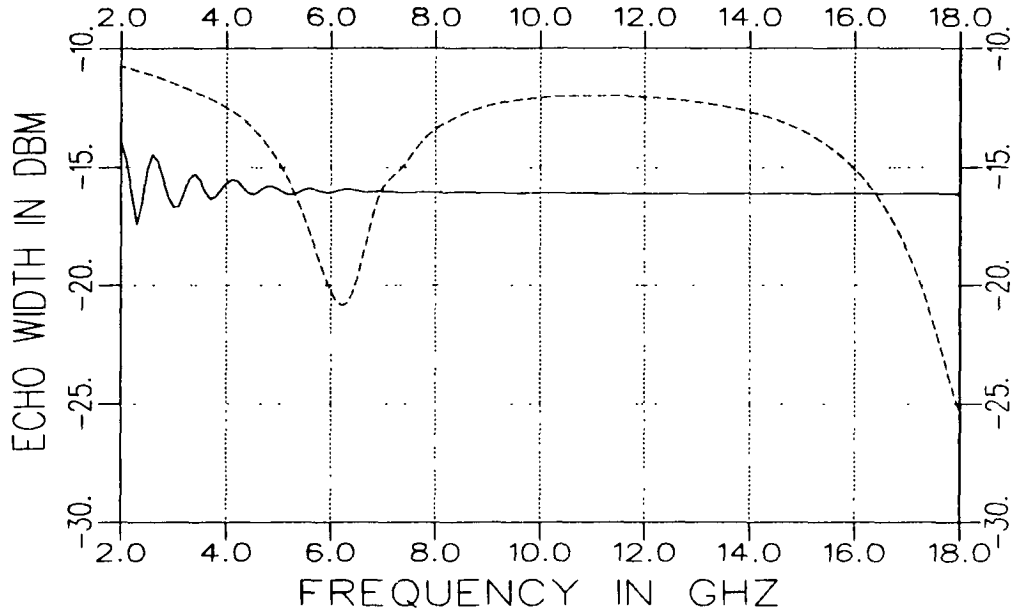


Figure 3.4: Swept frequency backscatter response for circular cylinders with $\epsilon_r = 24 - j2$ and $\mu_r = 2 - j2$. Solid line - 2" diameter homogeneous cylinder, dashed line - 2" diameter perfectly conducting cylinder with .07" thick dielectric coating.

plane is shown in Figure 3.6. The exact scattered far field for plane wave illumination can be calculated by using image theory which results in the sum of the backscattered and bistatic scattered fields for a sphere in free space. The scattered field for a hemisphere on a ground plane can be written in the following form for the two principal polarizations

$$E_{\theta} = E_{\theta}^{sphere}(\theta = 0) + E_{\theta}^{sphere}(\theta = 2\theta_0) \quad (3.4)$$

and

$$E_{\phi} = E_{\phi}^{sphere}(\theta = 0) - E_{\phi}^{sphere}(\theta = 2\theta_0) \quad (3.5)$$

where $E_{\theta,\phi}^{sphere}$ is the scattered field for a sphere in free space at a bistatic angle of θ_0 .

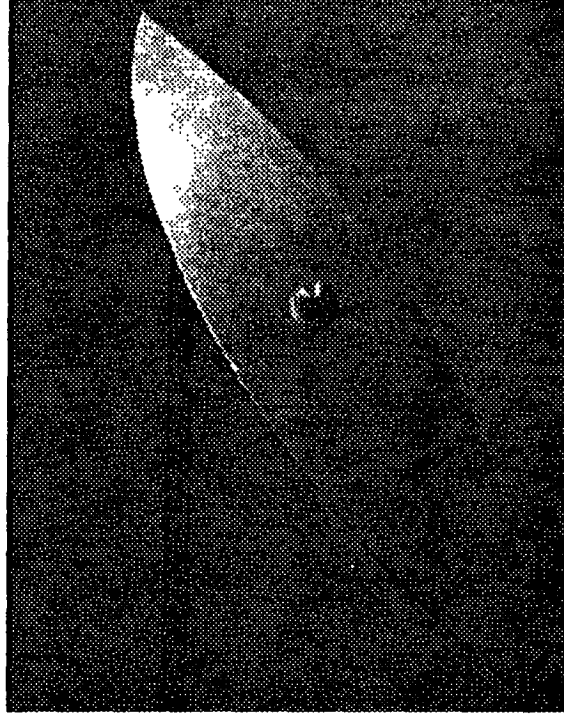


Figure 3.5: Ogival shaped ground plane fixture.

The scattered field expressions for a sphere in free space are given by
[3]

$$E_{\theta}^{sphere}(\theta) = -j \frac{E_o}{kr} e^{-jkr} \sum_{n=1}^{\infty} \left[b_n \sin \theta P_n^{1'}(\cos \theta) - c_n \frac{P_n^1(\cos \theta)}{\sin \theta} \right] \quad (3.6)$$

and

$$E_{\phi}^{sphere}(\theta) = -j \frac{E_o}{kr} e^{-jkr} \sum_{n=1}^{\infty} \left[b_n \frac{P_n^1(\cos \theta)}{\sin \theta} - c_n \sin \theta P_n^{1'}(\cos \theta) \right] \quad (3.7)$$

where $P^1(\cos \theta)$ and $P^{1'}(\cos \theta)$ are Legendre polynomials and

$$b_n = b_n^o \frac{B_n(A_n \mathcal{F}_n^1 - \eta_{r2} X_n \mathcal{F}_n^2)}{A_n(B_n \mathcal{F}_n^1 - \eta_{r2} X_n \mathcal{F}_n^2)} \quad (3.8)$$

and

$$c_n = c_n^o \frac{(X_n \mathcal{F}_n^3 - \eta_{r2} A_n \mathcal{F}_n^4)}{(X_n \mathcal{F}_n^3 - \eta_{r2} B_n \mathcal{F}_n^4)}. \quad (3.9)$$

where $\eta_{r2} = \sqrt{\frac{\mu_{r2}}{\epsilon_{r2}}}$ is the relative wave impedance of the material coating. The symbols b_n° , c_n° , A_n , B_n , X_n and $\mathcal{F}_n^{1,2,3,4}$ are ratios of spherical Bessel functions j_n and h_n given by

$$b_n^\circ = -\frac{2n+1}{n(n+1)} \frac{[kbj_n(kb)]'}{[kbh_n^{(2)}(kb)]'}, \quad (3.10)$$

$$c_n^\circ = -\frac{2n+1}{n(n+1)} \frac{j_n(kb)}{h_n^{(2)}(kb)}, \quad (3.11)$$

$$A_n = \frac{[kbj_n(kb)]'}{kbj_n(kb)} \quad (3.12)$$

$$B_n = \frac{[kbh_n^{(2)}(kb)]'}{kbh_n^{(2)}(kb)} \quad (3.13)$$

$$X_n = \frac{[k_1bj_n(k_1b)]'}{k_1bj_n(k_1b)} \quad (3.14)$$

$$\mathcal{F}_n^1 = F_n^1 - \frac{\eta_{r1}}{\eta_{r2}} \frac{[k_1aj_n(k_1a)]'}{[k_1aj_n(k_1a)]} \frac{[k_2ah_n^{(2)}(k_2a)]}{[k_2ah_n^{(2)}(k_2a)]'} F_n^4, \quad (3.15)$$

$$\mathcal{F}_n^2 = F_n^2 - \frac{\eta_{r1}}{\eta_{r2}} \frac{[k_1aj_n(k_1a)]'}{[k_1aj_n(k_1a)]} \frac{[k_2ah_n^{(2)}(k_2a)]}{[k_2ah_n^{(2)}(k_2a)]'} F_n^3, \quad (3.16)$$

$$\mathcal{F}_n^3 = F_n^3 - \frac{\eta_{r1}}{\eta_{r2}} \frac{[k_1aj_n(k_1a)]'}{[k_1aj_n(k_1a)]} \frac{[k_2ah_n^{(2)}(k_2a)]'}{[k_2ah_n^{(2)}(k_2a)]} F_n^2, \quad (3.17)$$

and

$$\mathcal{F}_n^4 = F_n^4 - \frac{\eta_{r1}}{\eta_{r2}} \frac{[k_1aj_n(k_1a)]}{[k_1aj_n(k_1a)]'} \frac{[k_2ah_n^{(2)}(k_2a)]'}{[k_2ah_n^{(2)}(k_2a)]} F_n^1. \quad (3.18)$$

where $\eta_{r1} = \sqrt{\frac{\mu_{r1}}{\epsilon_{r1}}}$ is the relative wave impedance and $k_1 = \sqrt{\epsilon_{r1}\mu_{r1}}k$ in the homogeneous sphere region, and $k_2 = \sqrt{\epsilon_{r2}\mu_{r2}}k$ with k being the free space wave number. The functions $F_n^{1,2,3,4}$ are ratios of spherical Bessel functions given by

$$F_n^1 = 1. - \frac{[k_1 a j_n(k_1 a)]'}{j_n(k_1 b)} \frac{h_n^{(2)}(k_1 b)}{[k_1 a h_n^{(2)}(k_1 a)]'}, \quad (3.19)$$

$$F_n^2 = 1. - \frac{[k_1 a j_n(k_1 a)]'}{[k_1 b j_n(k_1 b)]'} \frac{[k_1 b h_n^{(2)}(k_1 b)]'}{[k_1 a h_n^{(2)}(k_1 a)]'}, \quad (3.20)$$

$$F_n^3 = 1. - \frac{j_n(k_1 a)}{[k_1 b j_n(k_1 b)]'} \frac{[k_1 b h_n^{(2)}(k_1 b)]'}{h_n^{(2)}(k_1 a)} \quad (3.21)$$

and

$$F_n^4 = 1. - \frac{j_n(k_1 a)}{j_n(k_1 b)} \frac{h_n^{(2)}(k_1 b)}{h_n^{(2)}(k_1 a)}. \quad (3.22)$$

These above expressions also reduce to simpler forms for special cases. The $\mathcal{F}_n^{1,2,3,4}$ quantities reduce to $F_n^{1,2,3,4}$ for a perfectly conducting coated sphere, and $\mathcal{F}_n^1 = \mathcal{F}_n^2$ and $\mathcal{F}_n^3 = \mathcal{F}_n^4$ for a homogeneous dielectric sphere. Additionally, for the perfectly conducting sphere, $b_n = b_n^\circ$ and $c_n = c_n^\circ$.

The 2-18 GHz swept frequency backscatter response for a 2" diameter perfectly conducting hemisphere with an incidence angle of 30° from grazing is shown in Figure 3.7 where the solid curve is the theta polarized return case and the dashed is the phi polarized return case. These two cases are the nominal choices to acquire two independent measurements. Note that the responses at an elevation angle of 30° are reasonable for calibration references since they are fairly smooth for both polarizations. Figure 3.8 illustrates the backscatter, theta polarized frequency response for a homogeneous 2" dielectric hemisphere (solid line) and a 2" diameter perfectly

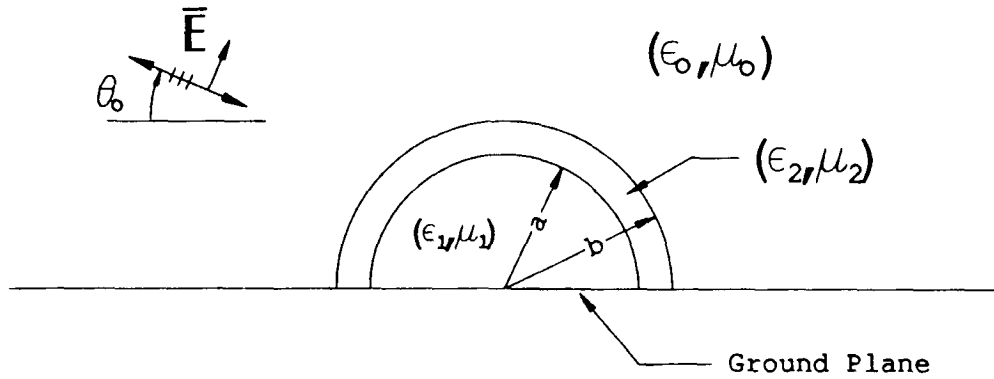


Figure 3.6: Geometry for a coated hemisphere.

conducting hemisphere coated with a .07" thick layer of dielectric. In both cases, the constitutive parameters are $\epsilon_r = 24 - j2$ and $\mu_r = 2 - j.2$. Similar comments can be made in regard to loss and material thickness for the hemispherical geometries as were made to the circular cylinder results shown in Figure 3.4. Also note that the calculations shown in Figure 3.8 were stopped at approximately 15 GHz due to the recursively generated Bessel functions used in the eigenfunction solution. Above this frequency for the chosen parameters, the Bessel function subroutines failed. For further calculations, the Bessel function values would have to be generated asymptotically.

III Sample Heating

Of the two fixtures, the ogival ground plane fixture would be the simplest to uniformly heat the material sample to the required temperatures. This conclusion is formed since the parallel plate fixture has more metal to heat to the desired temperature and keep heated to overcome the effective heat sink losses. Practical measurements with the ogival plate fixture would require that the heating be accomplished from the shadowed side of the ground plane and a metal curtain be formed around the perimeter of the ground plane to shield the heat source. The parallel plate fixture inherently

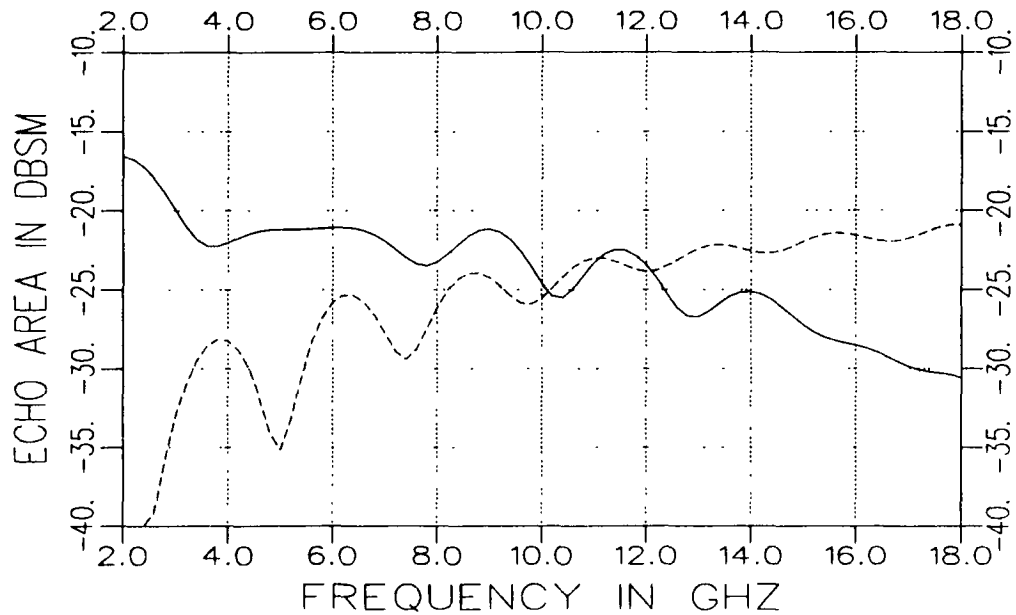


Figure 3.7: Swept frequency response for a 2" diameter perfectly conducting hemisphere with the incident field 30° from grazing incidence. Solid line - theta polarizatn, dashed line - phi polarization.

has a high degree of shielding from potential external disturbances. In both fixture designs, it is required that the samples be in good physical contact with the metal sides of the fixtures.

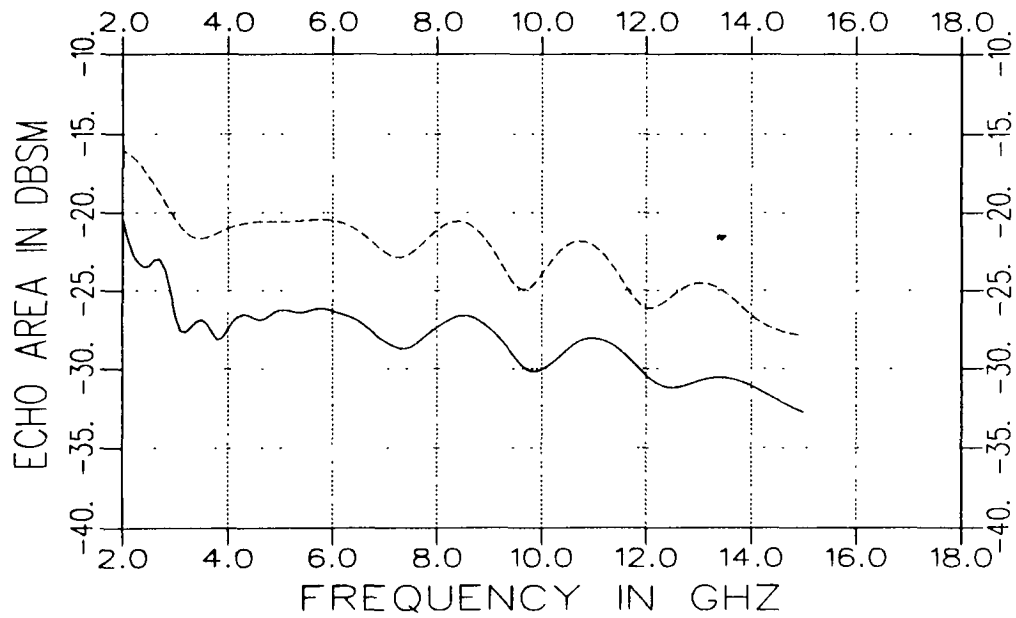


Figure 3.8: Swept frequency, theta polarized backscatter response for hemispheres with $\epsilon_r = 24 - j2$ and $\mu_r = 2 - j.2$. Solid line - 2" diameter homogeneous hemisphere, dashed line - 2" diameter perfectly conducting hemisphere with .07" thick dielectric coating.

Chapter 4

Example Measurements and Parameter Extraction

The examples that follow have been chosen to illustrate the concepts involved. The sample geometries measured were perfectly conducting and low loss dielectrics. Both fixtures were used to obtain the necessary measurements to extract the constitutive parameters for a lossy dielectric. All scattering calculations are normalized to echo width for the parallel plate measurements and echo area for the ground plane measurements. Echo width and echo area are respectively defined as

$$\sigma_W = 2\pi \lim_{\rho \rightarrow \infty} \rho \left| \frac{E^s}{E^i} \right|^2, \quad (4.1)$$

and

$$\sigma_A = 4\pi \lim_{r \rightarrow \infty} r^2 \left| \frac{E^s}{E^i} \right|^2 \quad (4.2)$$

The calibration technique of the measured data is very important. Equation 2.8 involves subtraction and multiplicative processes. The subtraction is to remove erroneous scattering terms present in the fixture. Figure 4.1 illustrates the backscatter terms present for the parallel plate waveguide in terms of a time signature. The waveform was generated by transforming

the swept frequency response using a fast Fourier transform when a 2" diameter disk was in the fixture. Figure 4.2 is a similar signature formed by subtracting the measurement with the disk absent in the fixture from the measurement with the disk present in the fixture. Note that many terms disappear but some do not since the fixture was slightly disturbed inserting and removing the sample. To remove the other error terms, soft time gating has to be employed by either the HP-8510B Network Analyzer or during the calibration process. It was found that better results were obtained by oversampling (smaller delta frequency increments) in the frequency domain and performing a software time gate on the data in the calibration process. A better signal to noise ratio can be obtained in the time domain by over sampling since the noise is spread throughout a larger time window.

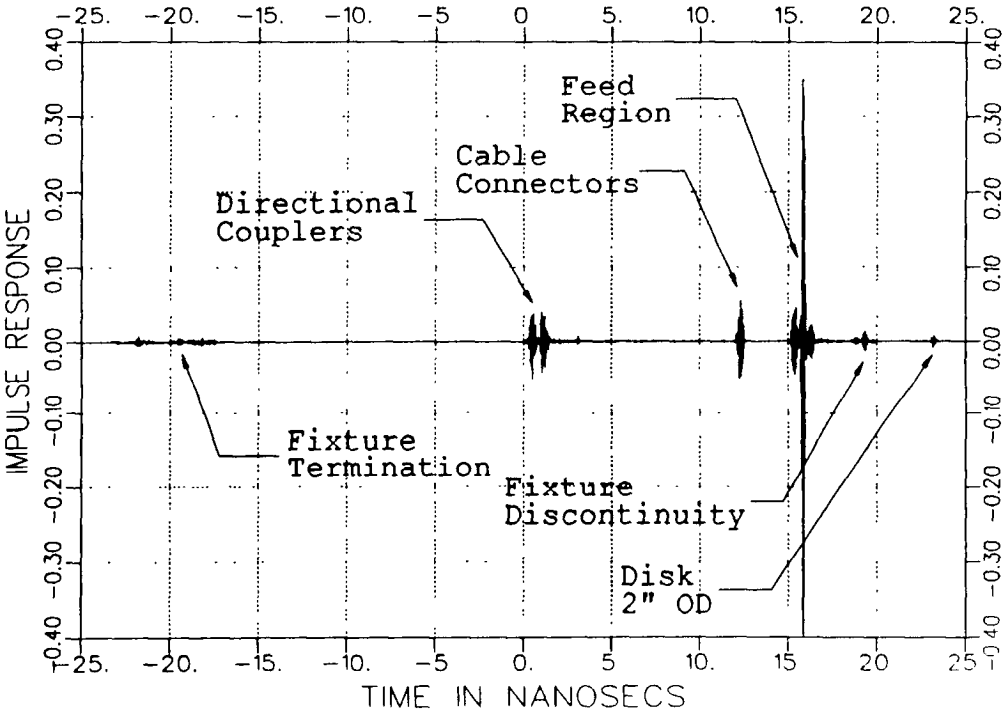


Figure 4.1: Scattering time signature of parallel plate fixture illustrating the scattering terms present for a reflection measurement.

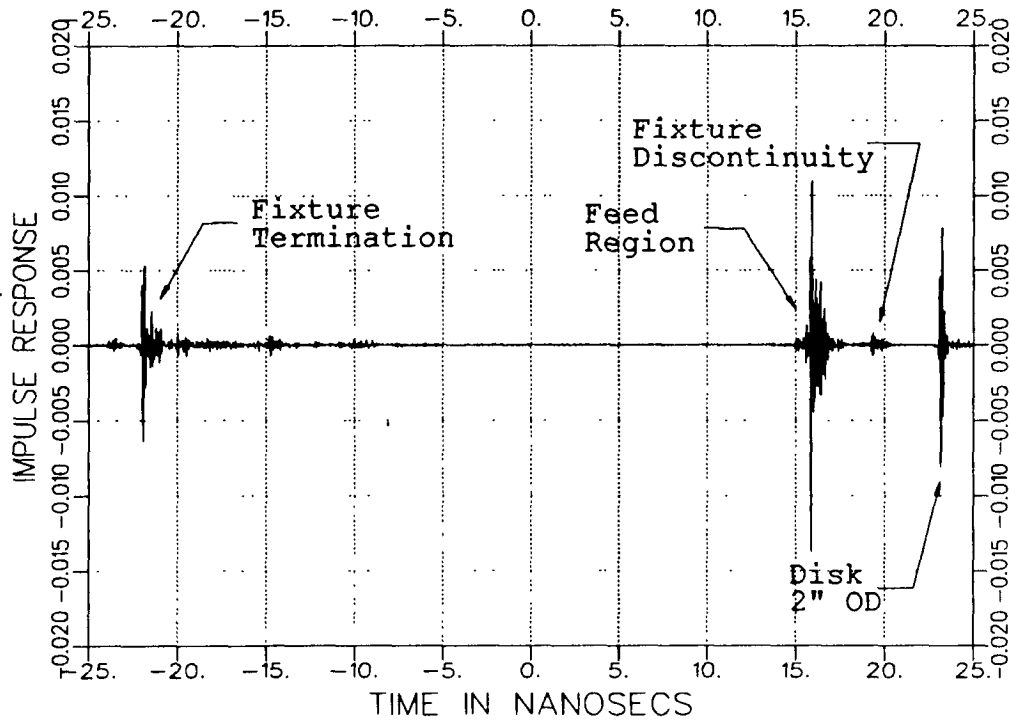


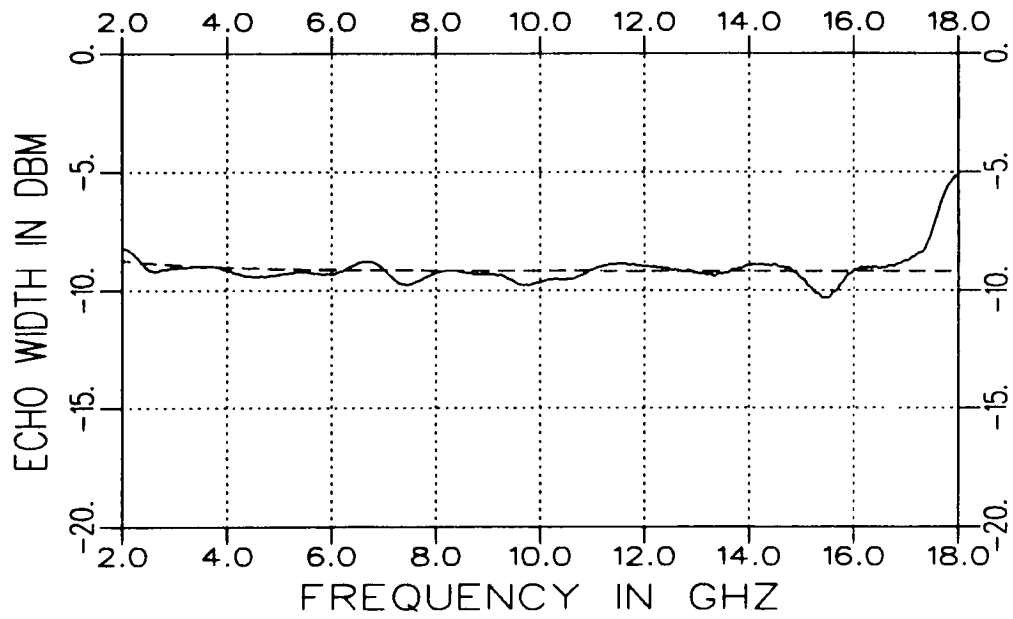
Figure 4.2: Scattering time signature of parallel plate fixture illustrating the scattering terms present for a reflection measurement after background subtraction.

The performance of the parallel plate fixture was evaluated by measuring a known sample. Figure 4.3 compares the measured and calculated responses for a 3" diameter, perfectly conducting, .313" thick disk at bistatic angles of 0° (backscatter) and 110° . Figure 4.4 shows the same measurement conditions for a 2" diameter Teflon disk. Figure 4.5 shows the extracted constitutive parameters as a function of frequency. The maximum variation around the mean value is approximately 2 %.

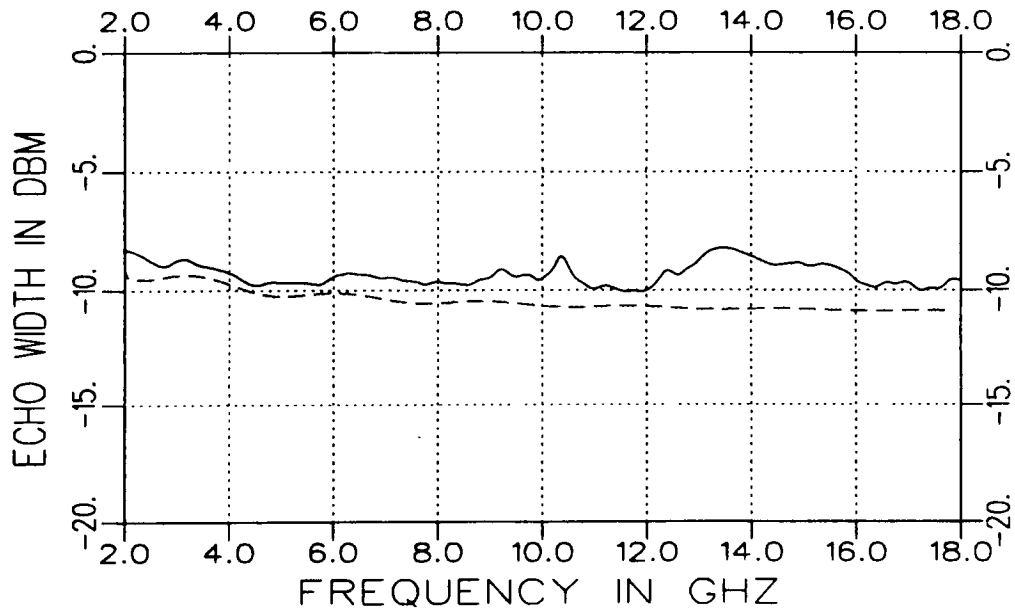
The performance of the ground plane fixture was evaluated by measuring a known sample. Figure 4.6 compares the measured and calculated responses for a 2" diameter, perfectly conducting hemisphere at an elevation angle of 30° from the ground plane for both principle polarizations. The performance of the system is good between 4 and 11 GHz. Figure

4.7 shows the same measurement for a 2" diameter Plexiglas hemisphere. Figure 4.8 shows the extracted constitutive parameters for this Plexiglas hemisphere as a function of frequency. As with the parallel plate fixture, the maximum variation around the mean value is approximately 2 %.

Other measurements were performed to observe the influence of a small gap between the ground plane and test samples. This gap would be desirable to concentrate the heat on the sample by providing an insulating air barrier to the metal ground plane. The measurements indicated substantial variations from the ideal situation for both incident polarizations such that no constitutive parameter extraction would be possible using the existing analytical model.



a



b

Figure 4.3: Parallel plate swept frequency results for a 3" diameter perfectly conducting disk: Solid - measured, dashed - calculated. a) Backscatter. b) bistatic, angle of 110°.

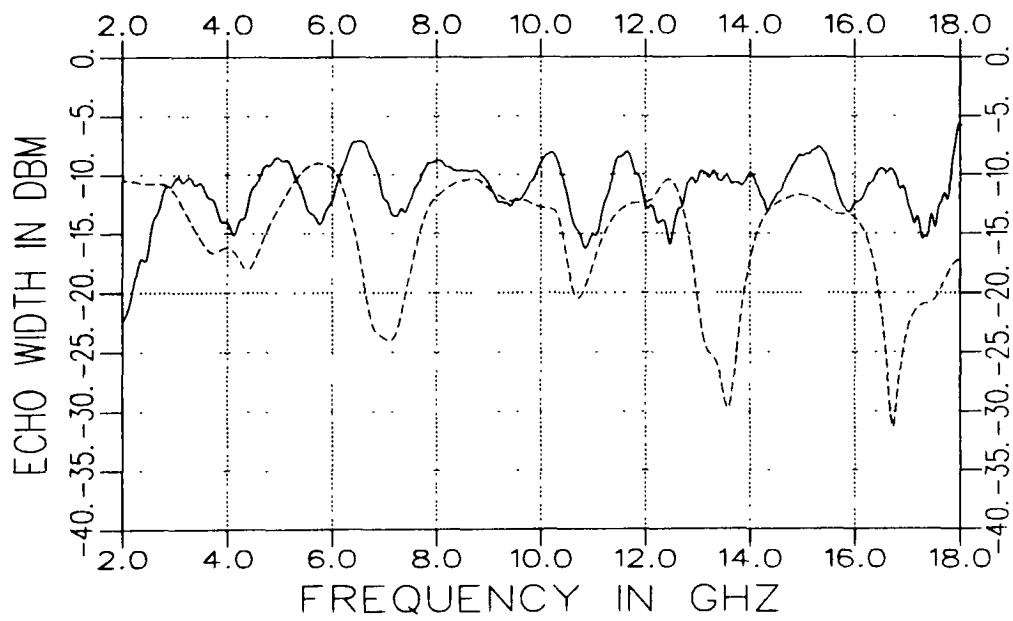


Figure 4.4: Measured parallel plate swept frequency results for a 2" diameter Teflon disk. Solid - backscatter, dashed - bistatic, angle of 110°.

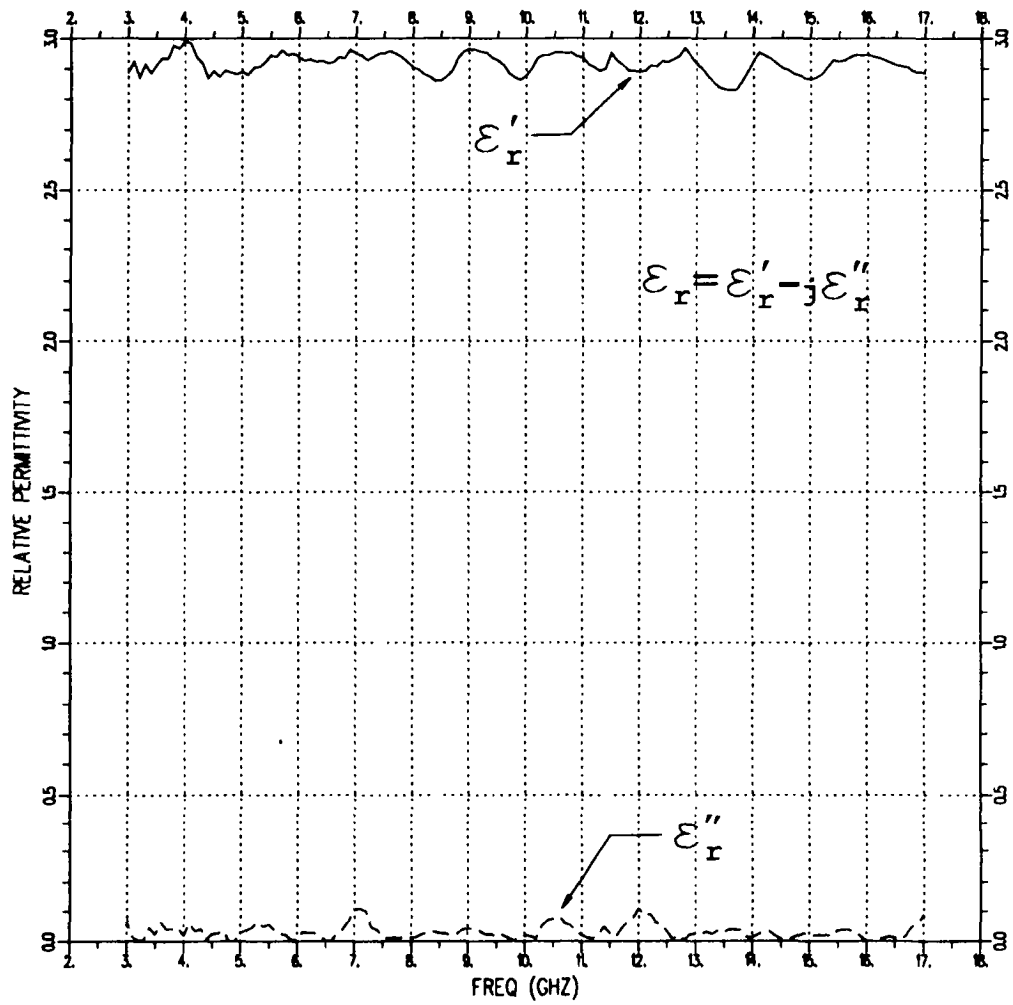
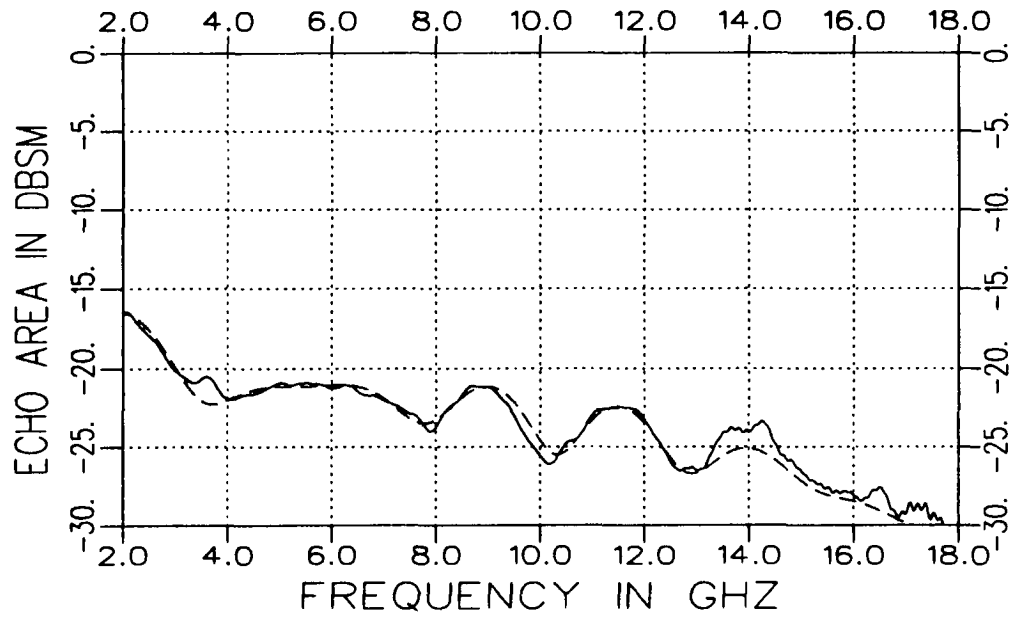
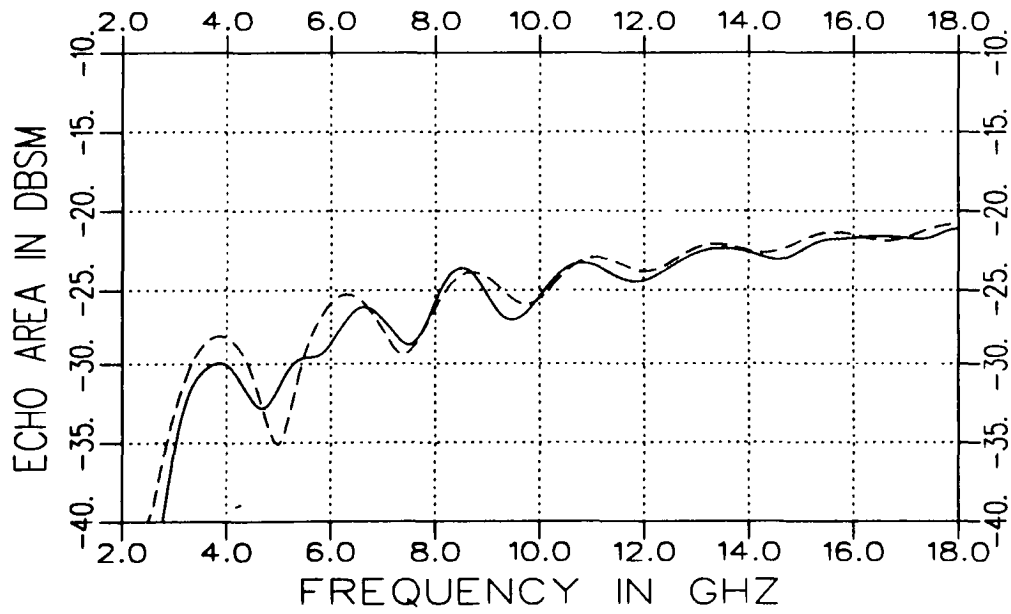


Figure 4.5: Extracted constitutive parameters for a 2" diameter Teflon disk.

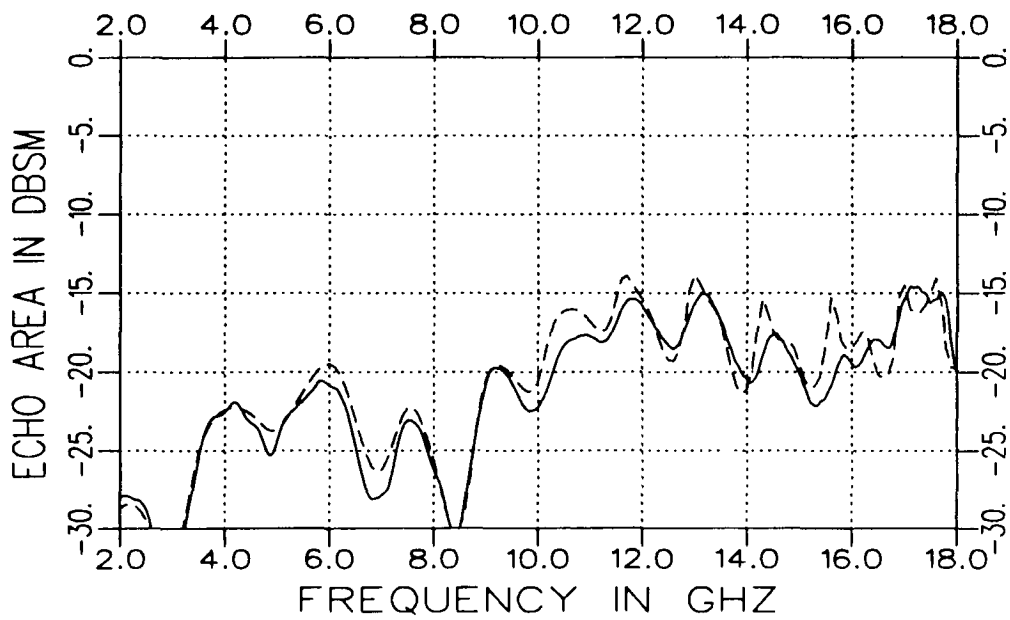


a

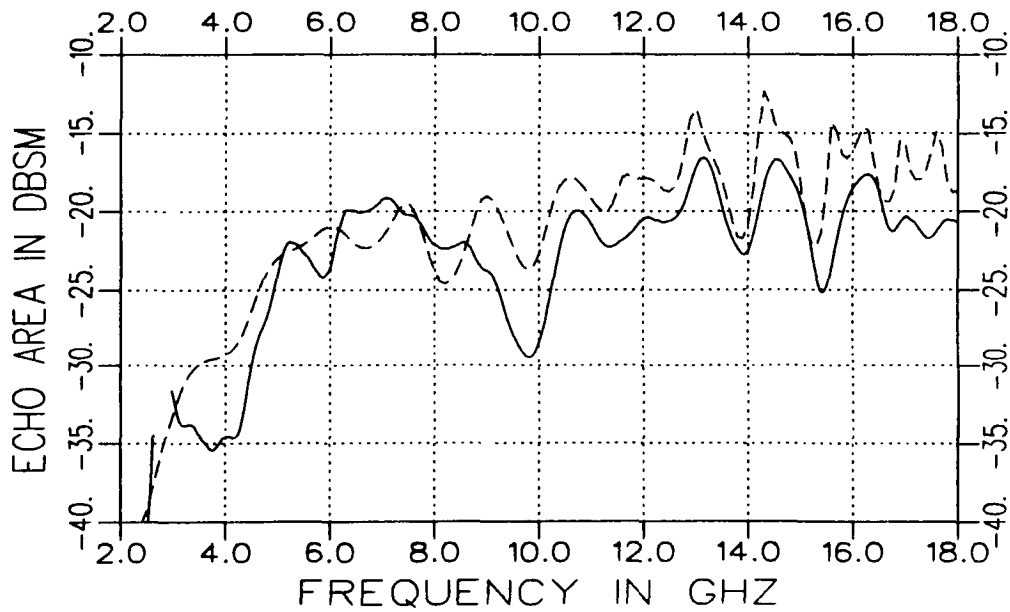


b

Figure 4.6: Ground plane swept frequency results for a 2" diameter perfectly conducting hemisphere, 30° from grazing: Solid - measured, dashed - calculated. a) Theta polarization. b) Phi polarization.



a



b

Figure 4.7: Measured ground plane swept frequency results for a 2" diameter Plexiglas hemisphere, 30° from grazing. Solid -theta polarization, dashed - phi polarization.

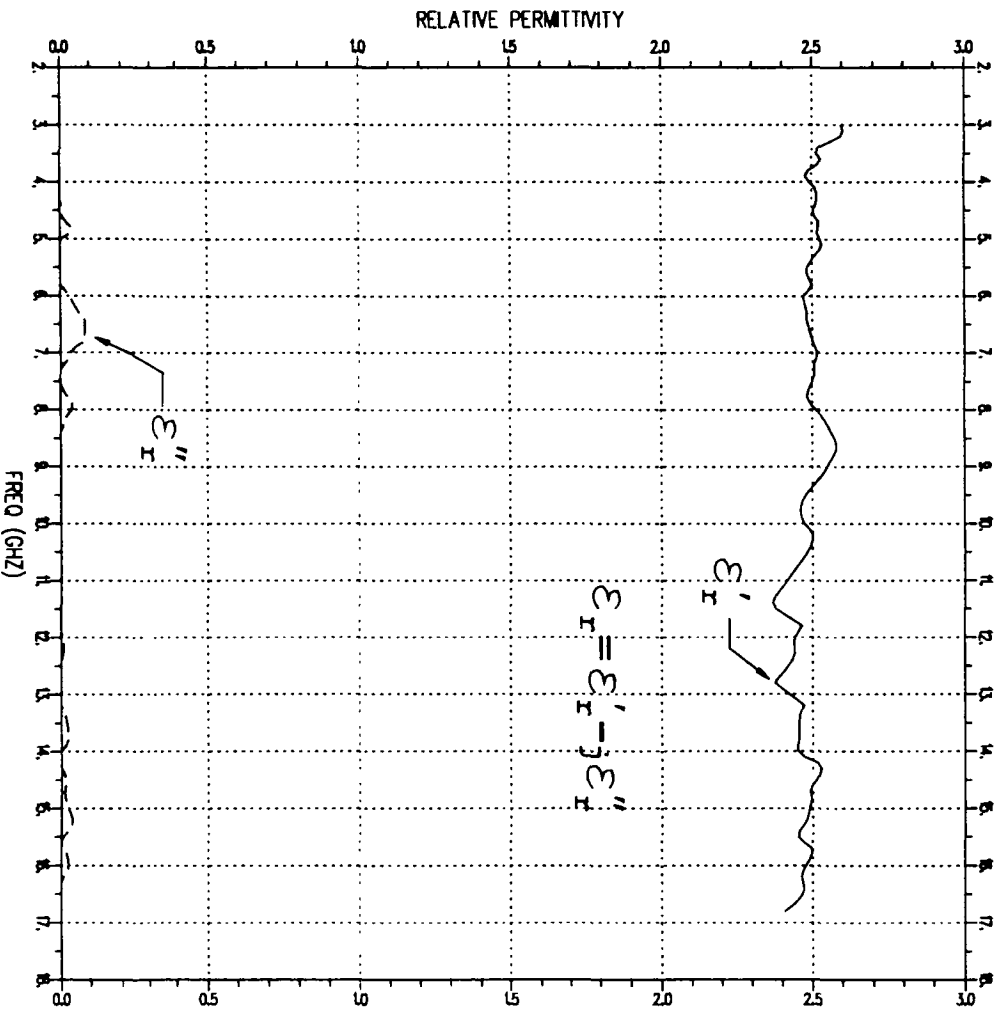


Figure 4.8: Extracted constitutive parameters for a 2" diameter Plexiglas hemisphere.

Chapter 5

Extraction Technique Sensitivity

The ability to extract the correct constitutive parameters from material measurements depends upon how well the fixture and sample geometry simulate the analytical model. Some differences between the physical and theoretical models can be tolerated. Errors originating from scattering due to fixture discontinuities can be minimized through processing measured data if the discontinuities occurred in a different physical location from where the sample was located. Errors originating from sample geometry differences such as incorrect dimensions can not be corrected.

An informative study to acquire tolerance limits on the extracted constitutive parameters is to extract these parameters from calculated swept frequency data assuming one of the geometry parameters is slightly different. Figure 5.1 illustrates the extracted parameters, normalized to the free space values, for a homogeneous dielectric, 2" diameter hemisphere with material parameters of $\epsilon_r = 2.6 - j0.$ and $\mu_r = 1. - j0.$. The incident field was theta polarized, 30° from grazing. The curves shown are for an assumed diameter of 1.96" and 2.04" for the perfectly conducting hemisphere. The maximum variation of the scattered field for these two cases was approximately 5 dB. The nominal measurement variation has been approximately 3 dB.

The influence of measurement processing is also of interest. Figure 5.2 shows a result of different smoothing of the backscattered swept frequency field for a 2" diameter Teflon disk in the parallel plate fixture as shown in Figure 4.4. The extracted relative permittivity is slightly dependent upon the degree of smoothing. Smoothing data with a moving average reduces noise and other scattering error terms. Note that a moving average is actually a discrete convolution and in the time domain it represents itself as a time gating window to remove terms outside the time region of interest.

Finally, the ability to extract large relative constitutive parameters through a search algorithm becomes more difficult as the the value becomes larger. The required accuracy of the measurements becomes very severe. Also as the loss becomes large, the functional dependence of the scattered field simplifies as shown in Figure 3.4 for the lossy homogeneous circular cylinder. This situation limits the extraction of parameters since all the scattered fields are basically described by a reflected field which is dependent upon only the ratio of ϵ and μ .

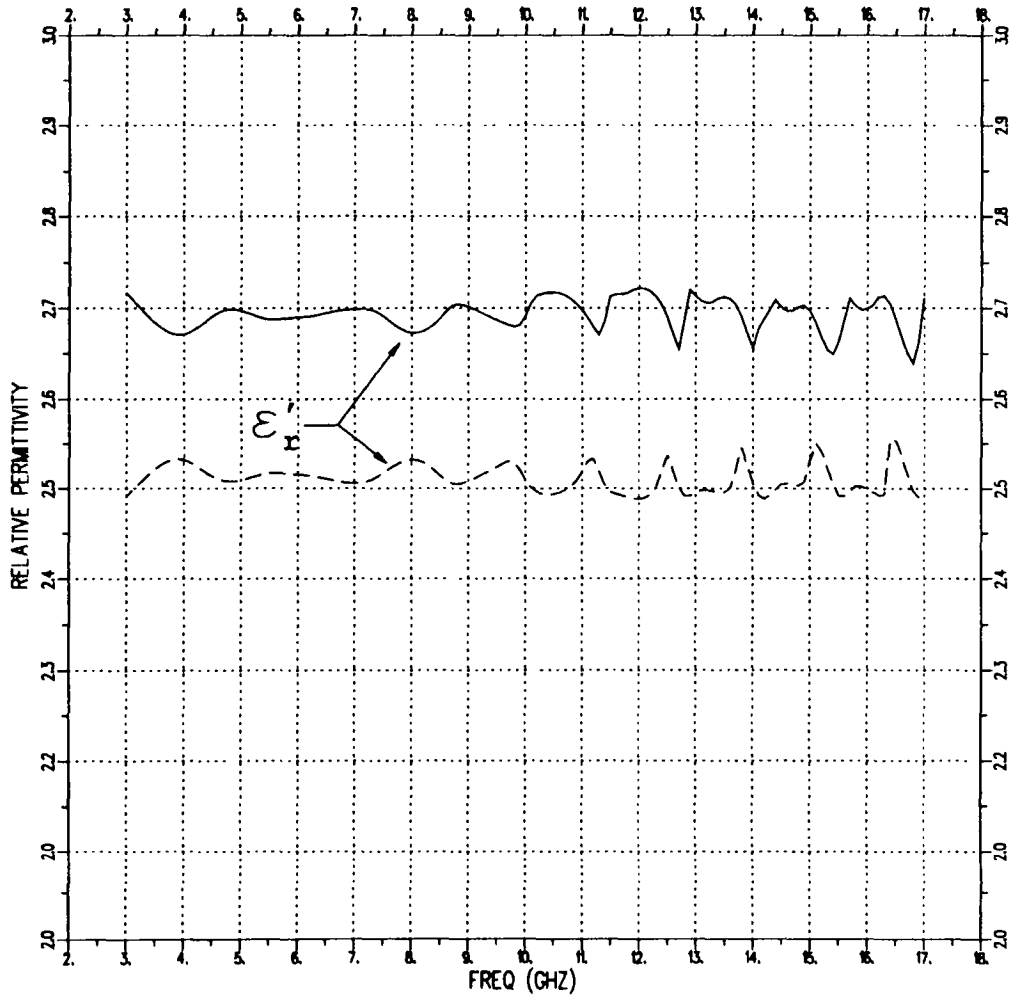


Figure 5.1: Normalized extracted constitutive parameters from calculated scattered field values. Assumed diameter for the perfectly conducting hemisphere: Solid line - 2 % smaller, dashed line - 2 % larger.

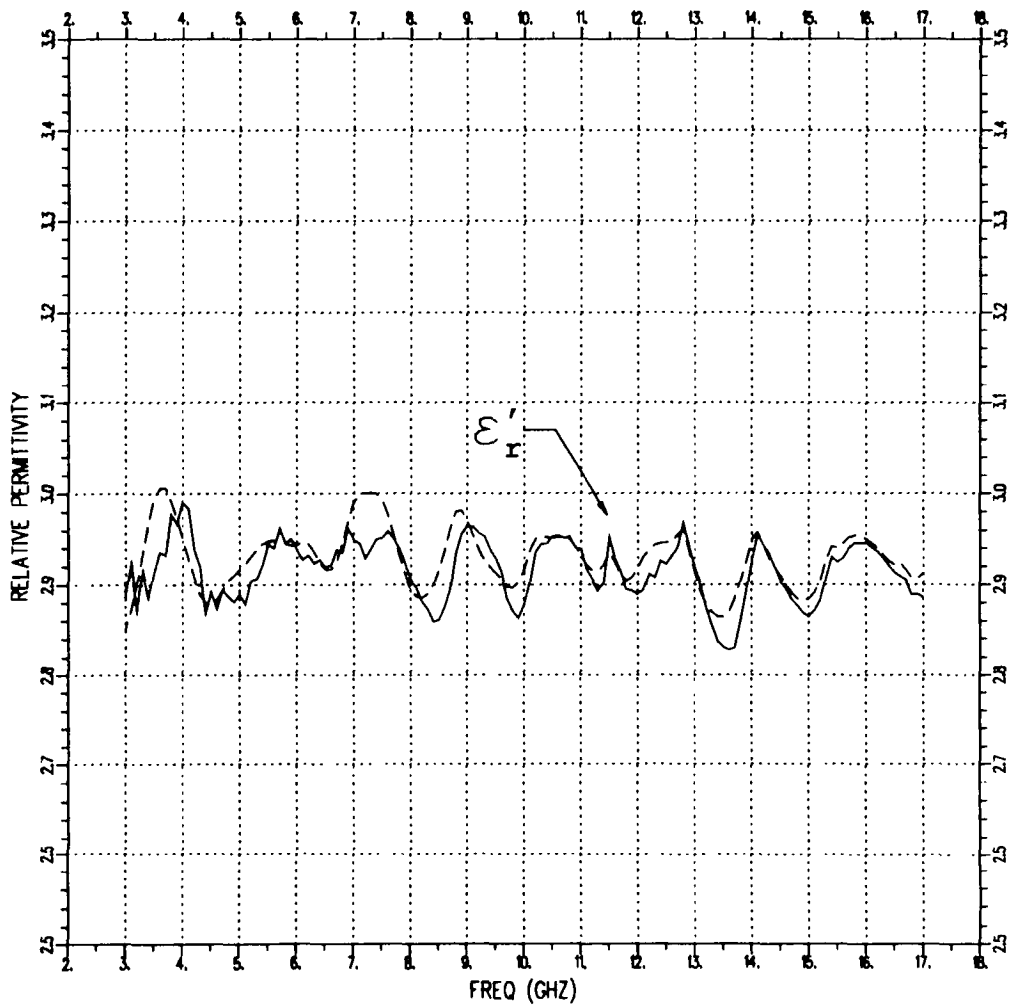


Figure 5.2: Backscattered results for a 2" diameter Teflon disk in the parallel plate fixture. Normalized extracted permittivity: Solid line - 31 points, dashed line - 71 points.

Chapter 6

An Alternate Fixture

The fixtures built and tested for parameter extraction were designed for broadband measurements using proven scattering techniques with a single fixture. Fabricating material samples in the required geometries demands care but such geometry sample shapes have been made in the past including spherical shapes. To achieve more accurate measurements than with these “free” space scattering approaches, the measurements have to be taken using a “non-radiating” fixture. The most common fixture incorporates a waveguide. However, the requirement of generating broadband measurements with a single fixture is then relaxed.

The conventional technique of waveguide reflection and transmission measurements can provide good signal to noise measurements. The standard sample approach is to have a sample which would completely fill the rectangular waveguide. The requirement of the sample completely filling the guide is based upon the equations used to extract the constitutive parameter values from the measurements. It is proposed to eliminate the requirement of having the sample completely fill the waveguide interior as shown in Figure 6.1. The sample would only partially fill the waveguide interior in one dimension. The proper set of equations would have to be developed for this geometry and a comparable Newton-Raphson technique could be used to extract the constitutive parameters. The sample geometry

has the convenience of being in a more readily fabricated shape and may be desirable since it is a planar coating which is closer to the final application form of the material. Such a fixture also has the advantage of providing high temperature measurements by placing a portion of the waveguide fixture in an oven. The actual design for a high temperature fixture would be different than the one shown in Figure 6.1 due to metal fatigue, oxidation and expansion considerations. Presently the sample holder concept would have to be changed since potential error terms can result from scattering due to the joints between the sample holder and the remaining fixture.

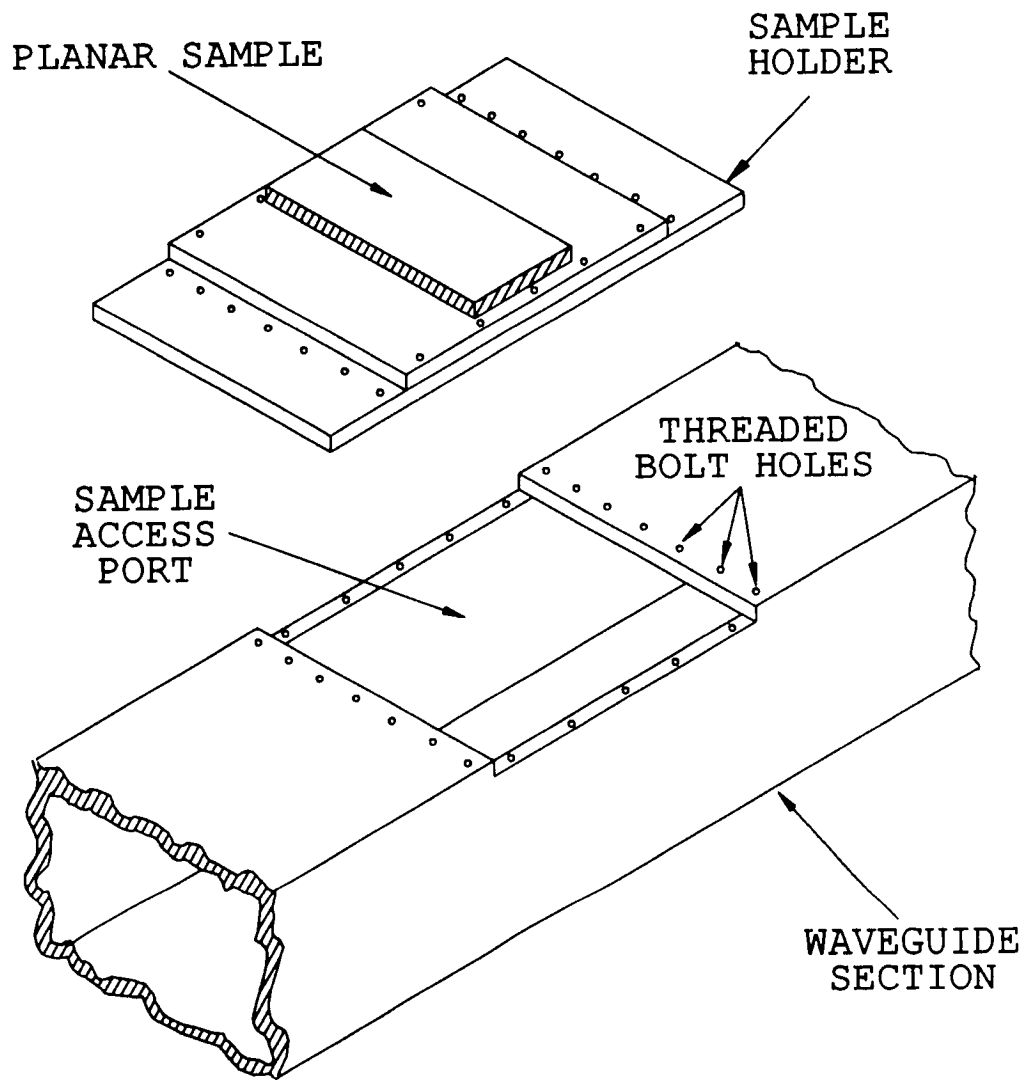


Figure 6.1: An alternate fixture using a rectangular waveguide fixture and a planar fixture sample.

Chapter 7

Conclusions

The wideband constitutive parameters were obtained for two generic geometries from scattered field measurements. A 2 % parameter variation was observed in the extracted parameters. The ability to acquire accurate enough measurements is the major electrical limitation for the presented technique. Software processing enhances the accuracy of the measurements by reducing the effect of fixture related error terms. An advantage of this approach over traditional waveguide techniques for material parameter measurements is that the material samples are free to expand for a given temperature. The actual high temperature sample dimensions could then be estimated from the room temperature dimensions using known coefficients of expansion. The ogival shaped ground plane fixture is more desirable over the parallel plate fixture for high temperature considerations of providing uniform heat to a small area with smaller fixture error terms to calibrate out.

To achieve more accurate measurements, a closed, nonradiating fixture may be considered as shown in Figure 6.1. Heating the fixture and sample becomes simpler. The sample geometry is also much easier to fabricate with a reduction in sample tolerances as compared to the traditional waveguide approach of filling the complete cross section with material.

Bibliography

- [1] Walton, E.K., M. Mittal, R. Slyh, and M. Poirier, "Development of an Advanced Microwave Free-Space Material Measurement System," ElectroScience Laboratory, Report No. 529696-1, July 1986.
- [2] Dominek, A., Park, A. and Peters, L., Jr., "Material Parameter Measurements at High Temperature," ElectroScience Laboratory, Report No. 719300-2, March 1988.
- [3] Young, J., "Constitutive Parameter Measurements Using the Scattering Technique," ElectroScience Laboratory, Report No. 1903-4, February 1967.
- [4] Yu, J.S. and Peters, L., Jr., "Measurement of Constitutive Parameters Using the Mie Solution of a Scattering Sphere," IEEE Proc., Vol. 58, No. 6, pp. 876-85, June 1970.
- [5] Hewlett Packard, "Measuring Dielectric Constant with the HP 8510 Network Analyzer," Product Note No. 8510-3.
- [6] Swarner, W.G., "Radar Cross Sections of Dielectric or Plasma Coated Conducting Bodies," ElectroScience Laboratory, Report No. 1116-21, August 1962.
- [7] American Electronic Laboratories, Inc., 305 Richardson Road, Lansdale, PA 19446.